Multicomponent ballistic transport in narrow single wall carbon nanotubes: Analytic model and molecular dynamics simulations

T. Mutat,[1] J. Adler,[1,a)] and M. Sheintuch[2]
[1]*Department of Physics, Technion, Haifa 32000, Israel*
[2]*Department of Chemical Engineering, Technion, Haifa 32000, Israel*

(Received 12 September 2010; accepted 3 December 2010; published online 27 January 2011)

The transport of gas mixtures through molecular-sieve membranes such as narrow nanotubes has many potential applications, but there remain open questions and a paucity of quantitative predictions. Our model, based on extensive molecular dynamics simulations, proposes that ballistic motion, hindered by counter diffusion, is the dominant mechanism. Our simulations of transport of mixtures of molecules between control volumes at both ends of nanotubes give quantitative support to the model's predictions. The combination of simulation and model enable extrapolation to longer tubes and pore networks. © *2011 American Institute of Physics*. [doi:10.1063/1.3532083]

I. INTRODUCTION

The transport of gas mixtures through molecular-sieve membranes and catalysts has been a subject of intensive interest due to many potential applications,[1–3] including hydrogen storage and separation.[4–7] In particular, issues concerning the diffusion of small molecules through carbon nanotubes (CNTs) are being studied for clean-energy production using relatively inexpensive membranes engineered from CNTs. Such separation involves several components and fluxes and is typically described by a Maxwell–Stefan (M–S) formalism.[8] Transport in narrow CNTs cannot be described by continuum diffusion concepts, since such diffusion is often of a single-file character with different characteristics to those of molecular diffusion. Molecular mechanics simulations[9] have shown that motion through a CNT may be almost ballistic in nature due to the smooth surface potential field. Other simulations and experiments have shown that such molecular transport can lead to extremely high apparent macroscopic diffusivities.[10–12]

Based on extensive molecular dynamics (MD) simulations of transport of small molecules through a narrow single wall carbon nanotubes (SWCNT), we have developed a theory of counter transport of single-file multicomponent transport applicable to pores that are smaller than about two molecular diameters. We consider only the rate through a single pore, allowing molecules to hop between two control volumes of constant chemical potential separated by a narrow SWCNT. We show that their transport probabilities can be described quite accurately by a new simple model that is markedly different from the M–S formalism, since it does not share the M–S assumption of linearity between the flux and the activity (i.e., concentration) gradient of all species.

As long as reliable quantitative analytical predictions for fluxes in these membranes were not developed, MD simulations remained the only valid tool for their study. Nonequilibrium molecular dynamics for diffusion in well-defined pores, such as CNTs, or in a porous layer have been extensively employed.[13] However, most previous computations were limited to small "samples," typically with one species, and to intermolecular potentials which were too simple to enable the results to be extended to more realistic situations. In a recent study,[14] we improved the potential quality by modeling both SWCNT and diffusive molecules with the more realistic Brenner reactive bond order (REBO) potential.[15] We carried out extensive tests to validate our code with single species transport and both flexible and rigid nanotubes. Our simulations of CH_4 inside fully flexible SWCNTs demonstrated that nanotube flexibility has a significant influence on transport diffusivity only at low pressure gradients. This observation is in agreement with those from Ref. 16. Although, this study was limited to the single species situation, we do not expect flexibility will change with more species present. More details about our simulation approach using REBO potentials and CH_4 transport in (12,12) and (10,10) SWCNTs were presented in Ref.14. The combination of our new extensive multicomponent simulations, with our new model which envisions ballistic motion hindered by counter diffusion, enable extrapolation of multicomponent transport simulation results to very long pores and to pore networks.

Motivation for this project stems from experimental measurements of multicomponent transport in a carbon membrane. The CNT can serve as a model for the carbon membranes which may be used in membrane reactors to enable hydrogen separation from hydrocarbons simultaneously with equilibrium-limited dehydrogenation reactions as reported in Ref. 17. We conclude with a comparison between our model predictions and these experimental measurements.

II. DETAILS OF OUR SYSTEM AND SIMULATION APPROACH

Since the interest is in high temperature applications, our simulations are carried out at 600 K. The short-range interactions of the covalent bonding between the carbon atoms in the SWCNT are calculated using the REBO potential. In the present study, the CH_4, H_2, and N_2 molecules

a)Electronic mail: phr76ja@tx.technion.ac.il.

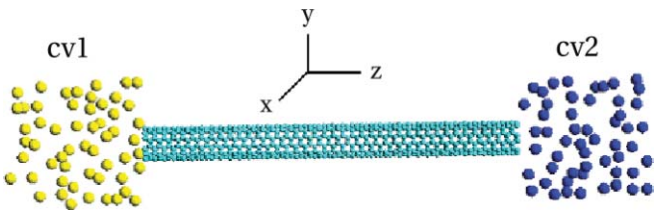

FIG. 1. Simulation system with white/black (yellow/blue online) molecules moving from CV1/CV2 through a nanotube of length L.

are treated as spherical particles with pairwise Lennard-Jones interactions between transporting molecules and the carbon atoms in the rigid SWCNT, with parameters taken from the literature.[18,19] As explained in more detail in Ref. 14, at the concentrations studied here, rigidity is not a drastic assumption. We implement the Dual Control Volume (DCV) grand canonical molecular dynamics (DCV-GCMD),[20] which combines grand canonical Monte Carlo simulations (GCMC) and MD methods. Using this technique, the SWCNT of length L (which is the flow region, oriented along the z axis) is bounded by two control volumes (CVs), CV1 on the left and CV2 on the right (see Fig. 1). The chemical potentials in the CVs are individually controlled by GCMC insertions and deletions of molecules, and their difference creates a gradient for MD flow through the tube.[21] The velocities of inserted molecules are determined by the Maxwell–Boltzmann distribution corresponding to the temperature set by the thermostat. Each DCV-GCMD cycle consists of 40–60 GCMC steps in the CVs followed by 1 MD step (with predictor corrector algorithm and a 0.5 fs timestep) in both the CVs and the flow region. This ratio is a good compromise between the need to keep the chemical potentials constant yet minimize computer time. Periodic boundary conditions are applied to the x and y directions (normal to the flow) for diffusive molecules in the CVs. Each CV is confined by two hard walls: on the outermost yx plane of the simulation volume and on the inner yx plane between the CV and the tube. This approach imitates a common experimental procedure used for the determination of diffusivities through porous materials.

We have conducted numerical experiments with single, binary, and ternary component mixtures of CH_4, N_2, and H_2 maintained in each CV to compute the average transport probabilities. Each simulation begins from a random configuration and is typically equilibrated for $10^6 - 3 \times 10^6$ GCMD cycles, followed by production times ranging from 10^6 to 7×10^6 cycles, depending on the tube loading. We define f_{ij} to be the number of molecules/s transported from control volume i to control volume j and f_{iN} to be the number of molecules/s entering the SWCNT (indicated by N) from control volume i. Note that $i, j = 1,2$, where the indices 1(2) indicate CV1(2). In all simulations presented below f_{iN} and f_{ij} are measured quantities, accumulated as the simulation progresses, rather than estimates from the kinetic theory of gases. Five different independent simulations were generated for each case with initial configurations and velocities generated using different random number seeds. Molecules were "tagged" with different colors, to monitor their actual flux. Visualizations with AViz (Ref. 22) were used to observe the nature of the flow. A selection of these can be viewed on our website.[23]

III. THE SINGLE-FILE TRANSPORT MODEL

Since single-file diffusion is a one-dimensional transport process in narrow pores where mutual passage of particles is excluded, its characteristics differ from ordinary diffusion; the mean square displacement of a molecule $< r^2 >$ is proportional to the square root of the diffusion time, t, through the tube, $< r^2 > \sim 2t^{1/2}$. For our case, where the motion is ballistic in nature, we built a simple model based on fast motion through a CNT. We developed an expression for the transport probability of a molecule through a SWCNT from CV1 to CV2 as a function of counter transport of molecules from CV2 to CV1 which is determined by the operating conditions. Our model describes situations where the density of gas in both CVs is relatively low, so that the tube has low occupancy. If the density was higher the tube is likely to be saturated with adsorbents.

We have developed analytic expressions for transport probability ratios such as f_{12}/f_{1N}. Ballistic motion of molecules from CV1 to CV2 which we will call "yellow" molecules as well as counter diffusion in the opposite direction of molecules that we will call "blue" ones, see Fig. 1, is assumed with no loss of energy and unchanged velocity distributions. The actual flux of yellow molecules is diminished due to counter transport: $f_{12} = f_{1N}\Theta$, where Θ is the transport factor. Now, the transport factor of yellow is the probability that a diffusing molecule will not encounter a blue in the pore. Defining v to be the molecule velocity, the flight time for a uniform temperature system is $\tau = L/v$. If $\tau_1(\tau_2)$ is the flight times of yellow(blue) molecules through the tube and f_{2N} is the entering frequency of counter molecules transporting from the right, then the probability of finding yellow(blue) molecules in the tube is $f_{1N}\tau_1(f_{2N}\tau_2)$, as long as $f_{2N}\tau_2 < 1$.

We first consider counter diffusion when both CVs contain the same molecular components at the same pressure. Here, the frequency of molecules (of mass m) entering the SWCNT from both CVs is equal ($f_{1N} = f_{2N}$) and $\Theta = 1 - 2f_{2N}(L/v)$. We develop an approximation to account for the distribution of velocities. Assuming that prior to collision the molecules have the same velocity as in the CVs, we define $v = v^*$ as the smallest velocity that will allow molecules to pass through the tube. At this threshold velocity $\Theta = 0$ or $v^* = 2f_{2N}L$; thus for $v > v^*$, $\Theta = 1 - v^*/v$. To evaluate the probability that a molecule transports from CV1 to CV2, we integrate over the whole distribution:

$$\frac{f_{12}}{f_{1N}} = \int_{v^*}^{\infty} \left[1 - \frac{v^*}{v}\right] g(v)dv \ , \tag{1}$$

where the velocity distribution function $vg(v)$ is obtained from the Maxwell–Boltzmann distribution, $g(E) = A\exp(-E/K_BT)$. Assuming one-dimensional motion of the molecules inside the tube, the expression becomes $g(v) = (2m/\pi K_BT)^{-1/2}\exp(-mv^2/2K_BT)$.

On changing the variable to kinetic energy, $E^* = mv^{*2}/(2K_BT)$, the equation above takes the form

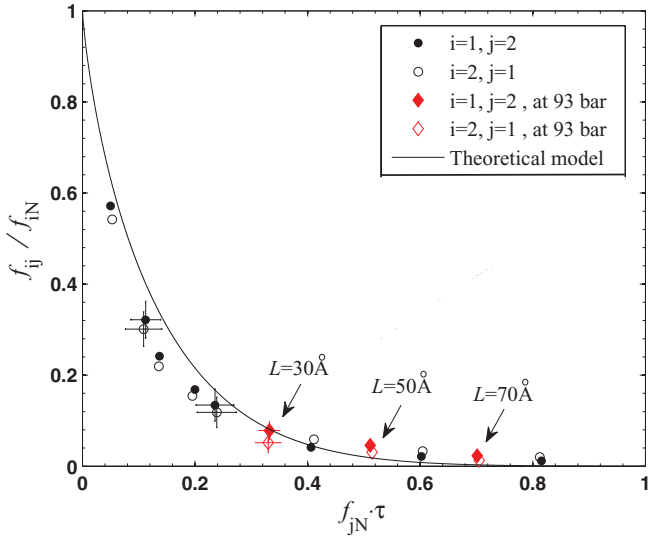

FIG. 2. Testing directional symmetry of single species transport with varying tube length. Transport probability of CH_4 from CV1 (CV2) to CV2 (CV1) vs counter diffusion of CH_4 through a (6,6) SWNT of L = 30, 50, and 70 Å and $P_{CV1} = P_{CV2}$ = 93 bars (red diamonds). Eight more simulations of CH_4 through a (6,6) SWNT (L = 100Å) are shown. Pressure values of $P_{CV1} = P_{CV2}$ = 10, 19, 23, 32, 37, 56, 74, 93 bars were given to both CVs and the results shown with black circular symbols with increasing pressures left to right on the figure. Error bars are shown on selected symbols. The solid curve represents the transport probability obtained from the single-file transport theory. This curve represents transport probability of molecules from CV1 to CV2 vs counter diffusion of molecules transporting from CV2 to CV1 for the case where $i = 1, j = 2$ and in the opposite direction for $i = 2$, $j = 1$.

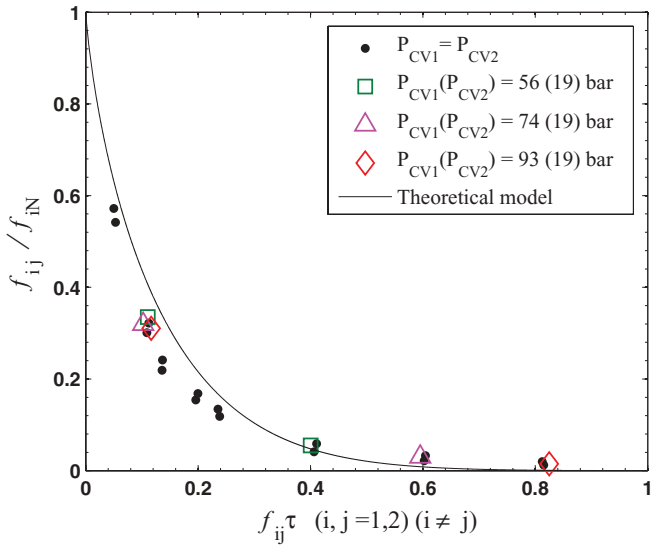

FIG. 3. Varying pressure: transport probability of CH_4 through a (6,6) SWNT (L = 100 Å) from CV1(CV2) to CV2(CV1) vs counter diffusion of CH_4 under pressure gradients (open symbols). Transport probabilities of CH_4 with $P_{CV1} = P_{CV2}$=10, 19, 23, 32, 37, 56, 74, 93 bars (were also shown in Fig. 2 are added for comparison (filled circles). The solid curve represents the transport probability obtained from the single-file transport theory.

$$\frac{f_{12}}{f_{1N}} = \frac{1}{\sqrt{\pi}} \int_{E^*}^{\infty} \left[\frac{1}{\sqrt{E}} - \frac{\sqrt{E^*}}{E} \right] \exp(-E) dE. \tag{2}$$

To find the threshold energy we need the average velocity, and for our one-dimensional motion the prefactor A is obtained by integrating $vg(v)$ from 0 to ∞ and normalizing to unity. The average velocity, derived from the kinetic theory of gases, at temperature T in the CV is given by

$$\langle v \rangle = \int_0^{\infty} v g(v) dv = \sqrt{\frac{8 K_B T}{\pi m}}\,. \tag{3}$$

Multiplying E^* by $\langle v \rangle^2 / \langle v \rangle^2$and substituting the expression developed above for v^*, the threshold value becomes $E^* = 16/\pi\ (f_{2N}\tau)^2$. Thus, f_{12} depends explicitly only on one parameter (E^*), which in turn depends on the dimensionless $f_{2N}\tau$, i.e., the bombardment frequency and the average residence time. This form of transport probability is plotted as the solid line in Fig. 2. In Secs. IV–VI, we present our simulation results. Figures 2–5 present transport probability ratios as a function of finding molecules in the tube, from both model and simulations.

IV. SINGLE SPECIES MODEL VALIDATION

First, we compare the single-file transport model curve with simulated results of single species transport. To show that the simulated system is symmetric to transport when both CVs are maintained in similar conditions, a rigid (6,6) SWCNT of L=100 Å and equal CH_4 pressures in both CVs was studied. The pressures ranged from 10 to 93 bars with results displayed in Fig. 2. In this case, it is clearly observed that f_{1N} and f_{2N} are approximately equal. As a result, $f_{12}/f_{1N} \approx f_{21}/f_{2N}$ and the two counter fluxes produce overlapping points. In order to examine the influence of the length of the flow region on the transport probability, three more (6,6) SWCNTs with different L for 93 bars were also considered and shown in Fig. 2. It can be seen that the transport probability decreases almost exponentially with increasing counter-diffusion parameter.

Next, three cases of L = 100 Å with different pressure gradients were investigated and observed to overlap with the no-gradient situation, as shown in Fig. 3. Specifically, for $P_1 > P_2$, we denote pairs of ratios as

$$\begin{aligned} F_a &= \frac{f_{12}}{f_{1N}}, \qquad \text{for } P_{CV1} = P_{CV2} = P_1, \\ F_b &= \frac{f_{12}}{f_{1N}}, \qquad \text{for } P_{CV1} = P_{CV2} = P_2, \end{aligned} \tag{4}$$

and

$$\begin{aligned} F_c &= \frac{f_{12}}{f_{1N}}, \qquad \text{for } P_{CV1} = P_1,\ P_{CV2} = P_2, \\ F_d &= \frac{f_{21}}{f_{2N}}, \qquad \text{for } P_{CV1} = P_1,\ P_{CV2} = P_2, \end{aligned} \tag{5}$$

then

$$\begin{aligned} F_c &\approx F_b, \\ F_d &\approx F_a. \end{aligned} \tag{6}$$

To clarify this further, let us consider one specific example of a CH_4 pressure gradient: P_{CV1}= 56 bars and P_{CV2} = 19 bars (indicated as two points of in Fig. 3). It can be observed that the transport probability, $F_c = f_{12}/f_{1N}$, is approximately equal

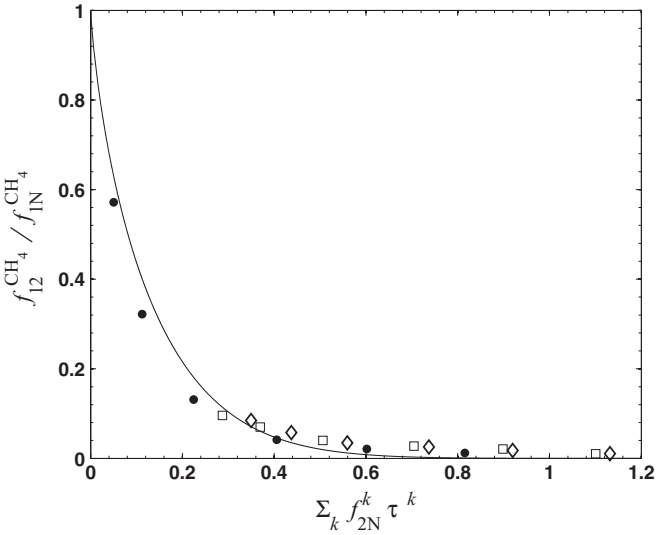

FIG. 4. Transport probability of CH_4 from CV1 to CV2 vs counter-diffusion parameter in a single-component system ($k = CH_4$) (●), in a bicomponent mixture ($k = CH_4$, N_2) (□), and in a triple-component mixture ($k = CH_4$, N_2, H_2) (◇). The pressure values are: $P_{CV1}^{CH_4} = P_{CV2}^{CH_4} = 10, 19, 37, 56, 74, 93$ bars. The partial fixed pressures are: $P_{CV1}^{N_2} = P_{CV2}^{N_2} = 37$ bars (in the binary and ternary cases) and $P_{CV1}^{H_2} = P_{CV2}^{H_2} = 19$ bars (in the ternary case). The solid curve represents the transport probability obtained from the single-file transport theory.

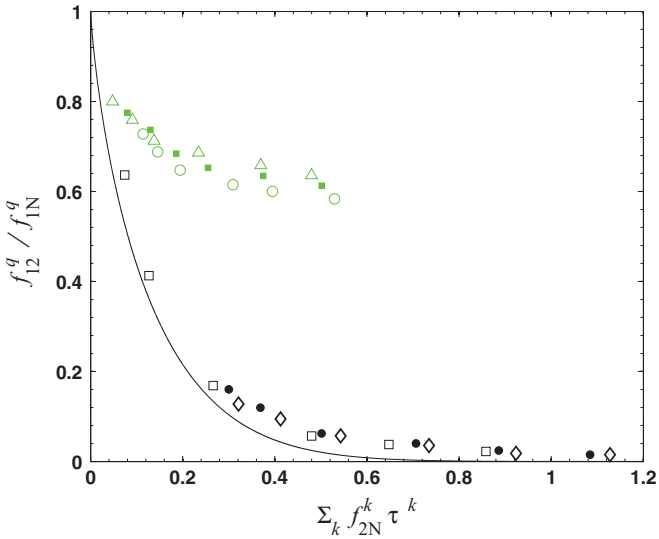

FIG. 5. Transport probability of $q = N_2$ from CV1 to CV2 vs counter-diffusion parameter, in a single-component system (k=N_2)□, in a bicomponent mixture ($k = N_2$, CH_4) (●), and in a triple-component mixture ($k = N_2$, CH_4, H_2) (◇). The pressure values are: $P_{CV1}^{N_2} = P_{CV2}^{N_2}$=10, 19, 37, 56, 74, 93 bars, partial pressures are: $P_{CV1}^{H_2} = P_{CV2}^{H_2} = 19$ bars, and $P_{CV1}^{CH_4} = P_{CV2}^{CH_4} = 37$ bars. The transport probability of $q = H_2$ in a single-component system ($k = H_2$) (△), in a binary mixture ($k = H_2$, CH_4) (■), and in a triple molecular mixture ($k = H_2$, CH_4, N_2) (○) are also shown. The pressure values are: $P_{CV1}^{H_2} = P_{CV2}^{H_2} = 10, 19, 37, 56, 74, 93$ bars, fixed partial pressures are: $P_{CV1}^{CH_4} = P_{CV2}^{CH_4} = 19$ bars and $P_{CV1}^{N_2} = P_{CV2}^{N_2} = 37$ bars. The solid curve represents the transport probability obtained from the single-file transport theory.

to F_b, the probability of molecules transporting when $P_{CV1} = P_{CV2} = 19$ bars. Furthermore, the transport probability of CH_4, $F_d = f_{21}/f_{2N}$, is approximately equal to F_a, the probability of molecules transporting when $P_{CV1} = P_{CV2} = 56$ bars. This indicates the dependence of the transport probability of molecules through the SWCNT on the counter diffusion..

V. EXTENSION TO MULTISPECIES TRANSPORT

The single-file model can be easily extended to molecules of different natures, in which case the molecular-weight-dependent average velocity should be modified. For the case of multicomponent single-file transport where mixtures of two or three gases in CV1(2) are kept at total pressure, $P_{CV1}(P_{CV2})$, the partial pressures of component k in each reservoir are denoted by $P_{CV1}^k(P_{CV2}^k)$. Both components can penetrate and diffuse through the SWCNT. As a result, they will exert mutual inhibition of the transport probability relative to its value for individual components. The expression for the transport factor should now include the inhibition factor due to all transporting molecules, as long as they are limited to single-file transport. Since we assume that on the average the density of particles is below unity, the inhibition to transport is additive and we can extend our expression for E^* by adding the various contributions, $E^* = \Sigma 16/\pi \left(f_{iN}^k \tau^k\right)^2$, where the two parameters, f_{iN}^k and τ^k, are those that describe the single-component system.

We evaluated the transport probability of CH_4 as a function of the counter-diffusion parameter of a bicomponent mixture (CH_4 and N_2) and of a ternary one with additional H_2 molecules. For both these cases, the CH_4 partial pressures were varied from 10 to 93 bars (compatible with those applied in the single-component simulations), while N_2 and H_2 pressures were kept fixed. As shown in Fig. 4 the transport probability values of CH_4 as a single component are considerably higher than the bi- and triple mixtures for the same CH_4 partial pressure. Furthermore, the transport probability values of CH_4 in the triple mixture are only slightly lower than in the bicomponent mixture with N_2. This suggests that the flux of CH_4 is significantly inhibited by the counter flow of large N_2 molecules and only slightly hindered by the small H_2 molecules.

Varying N_2 pressures while keeping CH_4 and H_2 pressures fixed, yielded similar results (Fig. 5). The transport probability values of N_2 as a single component are considerably higher than in a mixture with CH_4 for the same N_2 pressure. The transport probability values of N_2 in the triple mixture $CH_4/N_2/H_2$ are only slightly lower than in the binary with CH_4. This suggests that the flux of N_2 is significantly inhibited by the CH_4 and only slightly hindered by H_2 molecules.

In an intermediate summary we note that the simulated transport probabilities of the molecules diffusing as single component, binary, or ternary mixtures show good agreement with the theoretical model curve, over a domain of pressures and dimensions (Figs. 2–4 and the lower curve of Fig. 5). The observed hindrance of the molecules diffusing as molecular mixture through the tube is also predicted well by the model [Eq. (2)]. At this point, we note that some simulation values fall above the model curve and others below since the model does not explicitly allow for different molecular weights, but these, of course, influence the simulation results.

Due to its small size transport probabilities of H_2 are high when compared with those of CH_4 and N_2 and are not in agreement with the single-file curve (Fig. 5). The transport probabilities of H_2 as a single component are only slightly higher than the values in bi- and triple mixtures. These values indicate that the flux of H_2 in the (6,6) SWCNT is only slightly inhibited by the other molecules, since the small H_2 molecules can hop over CH_4 and N_2 molecules. Our visualizations[23] confirm that the CH_4 and N_2 follow single-file diffusion within the tube, whereas H_2 follows activated normal mode diffusion.

The counter-diffusion parameter of the molecular mixture (binary or triple) is approximately equal to the summation of its component counter-diffusion parameters if they were diffusing in a single-component system. For example, the value of the counter-diffusion parameter of the triple mixture $CH_4/N_2/H_2$ at a CV total pressure of 66 bars (Fig. 4, ◇) is approximately equal to the summation of CH_4, N_2, and H_2 diffusing in a single-component system at a CV pressure of 10 bars (Fig. 4, •), 37 bars (Fig. 5, □) and 19 bar (Fig. 5, △), respectively. Also, the counter-diffusion parameter of the triple mixtures is approximately equal to the counter diffusions of the bicomponent mixture together with the single component. In both cases the transport probability is strongly dependent on the counter diffusion.

VI. DISCUSSION AND CONCLUSION

We have developed a simple model that assumes ballistic motion, hindered by counter ballistic motion (diffusion), to describe the transport of gas mixtures through narrow CNTs, where molecules cannot bypass each other. The model predicts results validated by our simulations of transport of mixtures of molecules between control volumes at both ends of nanotubes. These results cannot be accounted for by available theories of multicomponent diffusion. Our interest in this problem stems from several suggested applications of CNT for gas separation as well as from the use of CNTs network as a model for molecular-sieve membranes, which has many potential applications.

We conclude this contribution with a comparison to the experimental transport coefficients (permeabilities) of various hydrocarbons, measured in carbon membranes with counter diffusion of nitrogen.[17,24] In that experiment, the membrane was exposed to a hydrocarbon stream on one side and to nitrogen stream on the other, and the coefficients were determined from the overall balance on the module. The observation from the experiment was that CH_4 transport was not inhibited, while that of C_2H_6, C_3H_8, C_4H_{10} was significantly inhibited by N_2 counter transport, and to a first approximation this inhibition is independent of the molecule as expected from the theory. Although the carbon membrane pore structure is more complex than parallel CNTs and remembering the average experimental pore size is 6 Å,[17] we still expect similar features to be dominant. Our simulations showed that hydrogen transport does not inhibit the hydrocarbon molecule transport. From our new model, we realize that inhibition is independent of the molecular nature with the exception of hydrogen. The important parameters are $f_{1N}\tau_1$ and $f_{2N}\tau_2$ which according to the kinetic theory of gases are independent of average velocity and, therefore, of pressure and molecule size. We can use the measured f_{12}/f_{1N} to estimate the effective pore length.

In summation: The single-file fluxes computed here show completely different scaling to that of the M–S formalism. They are not linear as a function of pressure drop, pore diameter, or inverse pore length, as would be the case for Fickian diffusion as reported in Refs. 25–27. The results of our simulations together with our model present a uniform picture of the transport nature of small molecules through narrow SWCNTs and the model enables extrapolation to longer systems. This picture is also in qualitative agreement with experimental results of transport through carbon membrane. Future work will extend these results to wider SWCNTs, in which some molecules may bypass others. A detailed discussion of the validity of this model will also be given there.

ACKNOWLEDGEMENTS

We acknowledge the HPC-EUROPA project for support of this work under Grants No. RII3-CT-2003-506079. T.M. acknowledges support from the Leonard and Diane Sherman Foundation.

[1] F. J. Keil, R. Krishna, and M. O. Coppens, Rev. Chem. Eng. **16**, 71 (2000).
[2] Z. F. Ren, Z. P. Huang, J. W. Xu, J. H. Wang, P. Bush, M. P. Siegal, and P. N. Provencio, Science **282**, 1105 (1998).
[3] S. K. Bhatia, Adsorpt. Sci. Technol. **24**, 101 (2006).
[4] A. C. Dillon, K. M. Jones, T. A. Bekkedahl, C. H. Kiang, D. S. Bethune, and M. J. Heben, Nature **386**, 377 (1997).
[5] G. Hummer, J. C. Rasaiah, and J. P. Noworyt, Nature **414**, 188 (2001).
[6] Q. Wang, S. R. Challa, D. S. Sholl, and J. K. Johnson, Phys. Rev. Lett. **82**, 956 (1999).
[7] T. D. Power, A. I. Skoulidas, and D. S. Sholl, J. Am. Chem. Soc. **124**, 1858 (2002).
[8] G. R. Gavalas, Ind. Eng. Chem. Res. **47**, 5797 (2008).
[9] A. I. Skoulidas, D. M. Ackerman, J. K. Johnson, and D. S. Sholl, Phys. Rev. Lett. **89**, 185901 (2002).
[10] T. W. Ebbesen, J. Phys. Chem. Solids **57**, 951 (1996).
[11] M. Eswaramoorthy, R. Sen, and C. N. R. Rao, Chem. Phys. Lett. **304**, 207 (1999).
[12] D. Ugarte, A. Châtelain, and W. A. de Heer, Science **274**, 1897 (1996).
[13] I. V. Kaganov and M. Sheintuch, Phys. Rev. E **68**, 46701 (2003).
[14] T. Mutat, "Atomistic simulation of diffusion and separation of small molecules in carbon nanotubes," M.Sc. thesis (Technion, 2007).
[15] D. W. Brenner, Phys. Rev. B **42**, 9458 (1990).
[16] S. Jakobtorweihen, M. G. Verbeek, C. P. Lowe, F. J. Keil, and B. Smit, Phys. Rev. Lett. **95**, 44501 (2005).
[17] G. A. Sznejer, I. Efremenko, and M. Sheintuch, AIChE J. **50**, 596 (2004).
[18] S. Gavalda, K. Gubbins, Y. H. K. Kaneko, and K. Thomson, Langmuir **18**, 2141 (2002).
[19] A. M. Vieira-Linhares and N. A. Seaton, Chem. Eng. Sci. **58**, 4129 (2003).
[20] G. S. Heffelfinger and F. van Swol, J. Chem. Phys. **100**, 7548 (1994).
[21] T. Düren, F. J. Keil, and N. A. Seaton, Mol. Phys. **100**, 3741 (2002).
[22] J. Adler, A. Hashibon, N. Schreiber, A. Sorkin, S. Sorkin, and G. Wagner, Comput. Phys. Commun. **147**, 665 (2002).
[23] See phycomp.technion.ac.il/~phr76ja/nanoflow.html.
[24] M. Sheintuch and I. Efremenko, Chem. Eng. Sci. **59**, 4739 (2004).
[25] L. Heinke, P. Kortunov, D. Tzoulaki, and J. Kärger, Phys. Rev. Lett. **99**, 228301 (2007).
[26] M. G. Clerc, E. Tirapegui, and M. Trejo, Phys. Rev. Lett. **97**, 176102 (2006).
[27] S. Gruener and P. Huber, Phys. Rev. Lett. **100**, 064502 (2008).